DOI: 10.1002/ejic.200500741

Tuning of the Spin States in Trinuclear Cobalt Compounds of Pyridazine by the Second Simple Bridging Ligand

Tao Yi*[a,b] Chang Ho-Chol,[b] Song Gao,[c] and Susumu Kitagawa*[b]

Keywords: Pyridazine/ Ligand tuning / Cobalt / Irregular spin states structure / Magnetic properties

Three novel trinuclear cobalt(II) compounds of pyridazine, $[Co_3(\mu\text{-}OH)_2(\mu\text{-}pdz)_4(pdz)_2(NO_3)_2(H_2O)_2]\cdot(NO_3)_2\cdot(THF)\cdot 2(MeOH)$ (**1**), $[Co_3(\mu\text{-}OH)_2(\mu\text{-}pdz)_4(pdz)_4(NO_3)_2]\cdot[Co_3(\mu\text{-}OH)_2(\mu\text{-}pdz)_4(MeOH)_4(NO_3)_2]\cdot(NO_3)_4$ (**2**), and $[Co_3(\mu\text{-}pdz)_4(\mu\text{-}NCS)_2(pdz)_2(NCS)_4]\cdot 2MeOH$ (**3**) (pdz = pyridazine), have been synthesized and characterized. The structures of all three compounds consist of centrosymmetric trimer building blocks bridged by the two nitrogen atoms of the pyridazine ligands and the second small bridging anions (hydroxide in **1** and **2**, and end-on thiocyanate in **3**). The two-atom bridging modes of the pyridazine ligand in **1** and **2** are unusual: each bridging pyridazine ligand affords two nitrogen donors to two metal ions with different bond lengths. This results in two kinds of spin states for the cobalt(II) atoms in **1**. Magnetic measurements show a typical antiferromagnetic interaction between the high-spin metals in **3**, but an unusual magnetic coupling through two high- and one low-spin cobalt atoms within the trimer in **1**. An irregular spin states structure is also observed in **1** at low temperature.

Introduction

Since the discovery of high-T_c magnetic molecular materials based on 3D metal-cyano compounds and the occurrence of the room-temperature, spin-crossover phase transition in 1,2,4-trizol compounds, strong magnetic interactions between two metal ions have played an important role in magnetic material chemistry.[1–4] Compounds with five-membered heterocyclic ligands such as 1,2,4-trizol attract much interest because of their special magnetic behavior, such as spin crossover,[4c] while the magnetic properties of diazine ligands are rarely considered to be important. Only a few examples of polynuclear copper(II) compounds of pyridazine (pdz)[5] and related ligands[6,7] have been structurally and magnetically characterized. Magnetic data and MO calculations indicate that the magnetic coupling of two metal ions in binuclear compounds of pdz always involves antiferromagnetic interactions through a short two-atom pdz exchange pathway.[8,9] However, in the trinuclear nickel(II) compound $[Ni_3(pdz)_6(\mu\text{-}SCN)_6]$,[10] for which the quasi Curie law magnetic behavior was published, the antiferromagnetic interaction through double pdz bridges was compensated for by the ferromagnetic interaction through a single end-on thiocyanato bridge. At that time, it was conjectured that the magnetic properties of such polynuclear systems could be tuned by the second bridging ligand. The cobalt ion would be a better magnetic center for this objective, because it has two spin states (high and low), depending only on its coordination environment.[11–12] Control of the cobalt(II) spin states by the choice of the axial ligand in pdz-bridged dicobalt(II) macrocyclic compounds has recently been reported by S. Brooker et al.,[13] whereas tuning of the spin states of metal ions through the different contributions of the two nitrogen donors of the pdz ligand by introducing a second bridging ligand has not been published yet. In this study, three novel trinuclear compounds bridged by the pdz ligand and a second bridging anion ($-OH^-$ or $-NCS^-$), $[Co_3(\mu\text{-}OH)_2(\mu\text{-}pdz)_4(pdz)_2(NO_3)_2(H_2O)_2]\cdot(NO_3)_2\cdot(THF)\cdot 2(MeOH)$ (**1**), $[Co_3(\mu\text{-}OH)_2(\mu\text{-}pdz)_4(pdz)_4(NO_3)_2]\cdot[Co_3(\mu\text{-}OH)_2(\mu\text{-}pdz)_4(MeOH)_4(NO_3)_2]\cdot(NO_3)_4$ (**2**), and $[Co_3(\mu\text{-}pdz)_4(\mu\text{-}NCS)_2(pdz)_2(NCS)_4]\cdot 2MeOH$ (**3**), have been isolated and characterized. In **1**, both triplet and singlet states of cobalt ions coexist within a trimer; an irregular spin states structure is observed at low temperature. The dominant magnetic interaction in **3** is antiferromagnetic.

Results and Discussion

Crystal and Molecular Structure of 1–3

Single crystals suitable for X-ray analysis were obtained, and the structure was characterized. Selected bond lengths and angles for the cobalt compounds **1**–**3**, as well as their crystallographic data are given in Table 1 and Table 2, respectively.

[a] Laboratory of Advanced Materials, Fudan University, Shanghai 200433, China
[b] Department of Synthetic Chemistry and Biological Chemistry, Faculty of Engineering, Kyoto University, Kyoto 606–8501, Japan
[c] State Key Laboratory of Rare Earth Materials Chemistry and Applications, Peking University, Beijing 100871, China

Table 1. Selected bond lengths and angles in **1**, **2**, and **3**.

Bond lengths [Å] of the central cobalt atom							
1		**2**				**3**	
		Trimer A		Trimer B			
Co2–O1	1.871(2)	Co1–O1	1.874(4)	Co4–O2	1.873(4)	Co1–N1	2.143(5)
Co2–N2	1.957(2)	Co1–N1	1.947(4)	Co4–N10	1.963(4)	Co1–N3	2.149(4)
Co2–N4	1.967(2)	Co1–N3	1.967(4)	Co4–N12	1.957(4)	Co1–N7	2.125(4)
Bond lengths [Å] of the terminal cobalt atoms							
1		**2**				**3**	
		Trimer A		Trimer B			
Co1–O1	1.968(2)	Co2–O1	1.996(4)	Co3–O2	1.970(4)	Co2–N2	2.192(4)
Co1–O2	2.098(3)	Co2–O5	2.092(4)	Co3–O3	2.093(4)	Co2–N4	2.195(5)
Co1–O3	2.061(2)	Co2–N2	2.139(5)	Co3–O4	2.104(6)	Co2–N5	2.174(6)
Co1–N1	2.130(2)	Co2–N4	2.176(4)	Co3–O8	2.039(7)	Co2–N7[d]	2.197(5)
Co1–N3	2.206(3)	Co2–N5	2.144(5)	Co3–N9	2.159(5)	Co2–N8	2.056(7)
Co1–N5	2.137(3)	Co2–N7	2.143(5)	Co3–N11	2.206(5)	Co2–N9	2.041(5)
Co1···Co2	3.24	Co1···Co2	3.24	Co3···Co4	3.23	Co1···Co2	3.45
Bond angles [°] of the central cobalt atom							
1		**2**				**3**	
		Trimer A		Trimer B			
O1–Co2–N4[a]	91.5(1)	O1–Co1–N1	88.1(2)	O2–Co4–N10	89.8(2)	N1–Co1–N3[d]	88.0(2)
N2–Co2–N4	91.05(9)	O1–Co1–N1[b]	91.9(2)	O2–Co4–N10[c]	90.2(2)	N1–Co1–N7	94.1(2)
N2–Co2–N4[a]	88.95(9)	O1–Co1–N3	89.0(2)	O2–Co4–N12	87.8(2)	N1–Co1–N7[d]	85.9(2)
		O1–Co1–N3[b]	91.0(2)	O2–Co4–N12[c]	92.2(2)	N3–Co1–N7	91.5(2)
		N1–Co1–N3	92.7(2)	N10–Co4–N12	92.1(2)	N3–Co1–N7[d]	88.5(2)
		N1–Co1–N3[b]	87.3(2)	N10–Co4–N12[c]	87.9(2)	N1–Co1–N3	92.0(2)
Bond angles [°] of the terminal cobalt atoms							
1		**2**				**3**	
		Trimer A		Trimer B			
O1–Co1–N5	95.39(9)	O1–Co2–O5	174.3(2)	O2–Co3–O3	95.8(2)	N2–Co2–N4	88.8(2)
O2–Co1–O3	88.19(9)	O1–Co2–N2	81.6(2)	O2–Co3–O4	93.3(2)	N2–Co2–N5[d]	94.0(2)
O2–Co1–N1	177.1(1)	O1–Co2–N4	81.5(2)	O2–Co3–O8	174.7(2)	N2–Co2–N7[d]	83.5(2)
O2–Co1–N3	95.9(1)	O1–Co2–N5	97.5(2)	O2–Co3–N9	83.2(2)	N2–Co2–N8	89.9(2)
O2–Co1–N5	92.0(1)	O1–Co2–N7	94.0(2)	O2–Co3–N11	80.2(2)	N2–Co2–N9	174.3(3)
O3–Co1–N1	90.79(9)	O5–Co2–N2	99.5(2)	O3–Co3–O4	92.6(2)	N4–Co2–N7[d]	86.0(2)
O3–Co1–N3	89.69(9)	O5–Co2–N4	93.0(2)	O3–Co3–O8	87.5(2)	N4–Co2–N8	89.7(2)
O3–Co1–N5	93.1(1)	O5–Co2–N5	88.1(2)	O3–Co3–N9	175.0(2)	N4–Co2–N9	88.0(2)
N1–Co1–N3	81.42(9)	O5–Co2–N7	85.1(2)	O3–Co3–N11	89.7(2)	N5–Co2–N7[d]	95.3(2)
N1–Co1–N5	90.7(1)	N2–Co2–N4	85.0(2)	O4–Co3–O8	82.4(3)	N5–Co2–N9	89.3(2)
		N2–Co2–N5	89.6(2)	O4–Co3–N9	92.3(2)	N7[d]–Co2–N8	172.2(2)
		N2–Co2–N7	174.9(2)	O4–Co3–N11	173.3(2)	N7[d]–Co2–N9	91.6(2)
		N4–Co2–N5	174.6(2)	O8–Co3–N9	93.8(2)	N8–Co2–N9	94.8(2)
		N4–Co2–N7	97.0(2)	O8–Co3–N11	104.0(2)	N5–Co2–N7[d]	95.3(2)
		N5–Co2–N7	88.4(2)	N9–Co3–N11	85.3(2)	N5–Co2–N8	89.3(3)
Bond angles [°] of cobalt atoms with bridging OH, SCN, and pdz							
1		**2**				**3**	
		Trimer A		Trimer B			
Co1–O1–Co2	114.8(1)	Co1–O1–Co2	113.7(1)	Co3–O2–Co4	114.3(2)	Co1–N7–Co2[d]	105.1(2)
Co1–N1–N2	119.9(2)	Co2–N2–N1	117.6(3)	Co3–N9–N10	116.2(3)	Co1–N1–N2	118.9(3)
Co2–N2–N1	117.6(2)	Co1–N1–N2	117.2(3)	Co4–N10–N9	118.1(3)	Co2–N2–N1	118.6(4)
Co1–N3–N4	115.8(2)	Co2–N4–N3	117.0(3)	Co3–N11–N12	116.4(3)	Co1–N3–N4	117.2(4)
Co2–N4–N3	118.0(2)	Co1–N3–N4	117.4(3)	Co4–N12–N11	117.3(3)	Co2[d]–N4–N3	120.3(3)

[a] $1 - x, -y, 1 - z$. [b] $1 - x, 1 - y, 1 - z$. [c] $-x + 1/2, -y + 1/2, -z + 1/2$. [d] $-x, -y, -z$.

Compounds **1** and **2** (Figure 1 and Figure 2, respectively) have centrosymmetric linear structures. The central cobalt ion lies on a crystallographic inversion center of a generic octahedral coordination sphere. In **1**, there is only one kind of trimer, as observed in most trinuclear compounds, while in **2**, there are two different trimers (**2**A and **2**B). In every trimer of both compounds, the three cobalt atoms are linked together by four μ-pdz ligands and two μ-OH groups. The coordination environments of the central cobalt atoms are the same. The strong electronegativity of oxygen results in only 1.87 and 1.962 Å for the average lengths of the bonds between the central cobalt atom and its bridging OH and pdz ligands, respectively. Differing from the pdz compounds published previously,[5–9,13–15] the bridging pdz ligands in **1** and **2** afford two nitrogen donors to the two adjacent metal atoms with quite different bond lengths, an

average of 1.96 Å to the central and 2.17 Å to the terminal cobalt atoms. The bridging OH group also affords different bond lengths to the central (average 1.87 Å) and terminal cobalt atoms (average 1.98 Å). It is interesting that the average bond length of the central cobalt atom is 1.93 Å, which is shorter than that of the terminal cobalt atoms (2.09 Å), but similar to that of the low-spin-state cobalt(II) atoms in diazide derivatives.[13] A significant contribution to these differences comes from the two nitrogen donors of the bridging pdz ligands. All of the terminal cobalt atoms in **1** and **2** are coordinated with two bridging pdz ligands and one bridging OH group. The other three positions are occupied by one monodentate pdz ligand, one NO_3^- ligand, and one water molecule in **1**, two terminal pdz ligands and one NO_3^- ligand in **2**A, and one NO_3^- ligand and two methanol molecules in **2**B. The angles subtended at the terminal cobalt(II) centers are 81.4(1)–95.9(1) in **1** and 81.5(2)–99.5(2) in **2**, whereas these angles are 88.95(9)–91.5(1) and 87.3(2)–92.7(2), very close to 90°, for the central cobalt(II) atoms of **1** and **2**, respectively, which indicates that the octahedral environment of the terminal cobalt centers is more distorted than that of the central one. The same situation was also observed when comparing the high-spin (HS) and low-spin (LS) cobalt compounds described in ref.[13]. By examining the structural information above, it can be postulated that the difference in the spin states of the central and terminal cobalt atoms is due to the varying strength of the ligand field around the two types of cobalt atoms. This is also proved by the magnetic data. The distance between the neighboring cobalt atoms in each trimer of both **1** and **2** is only 3.24 Å, much shorter than those in other pyridazine compounds.[13,14] The shortest intermolecular Co···Co distance is 7.04 Å. In **1**, there are two uncoordinated NO_3^- groups per trimer in the structure. Each one affords two oxygen atoms to connect the terminally coordinated water molecules of two neighboring trimers by hydrogen bonds with the following distances and angles: 2.718(3) Å and 171(4)° (O2–H18···O6), and 2.782(4) Å and 170(4)° [O2–H19···O8# (#: $1 - x$, $-y$, $1 - z$)]. The trimers are connected together, forming a two-dimensional folded sheet structure through hydrogen bonds along the *bc* plane. Compound **2** contains three uncoordinated NO_3^- counterions per trimer, but without intermolecular interactions. It should be noted that it is not common to have two different trimers in one crystal. The central cobalt atom in trimer **2**A occupies a central position of the cell, while that in trimer **2**B is at a corner position of the cell.

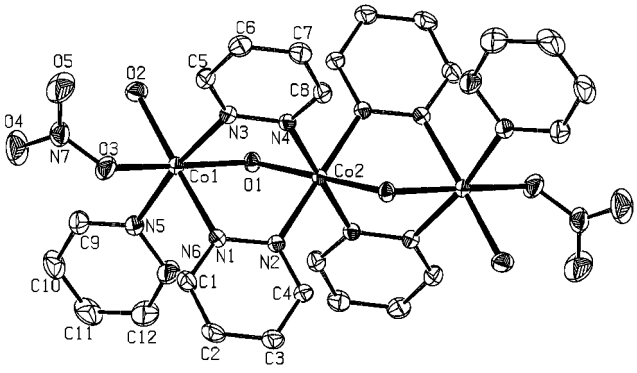

Figure 1. An ORTEP drawing of **1**, with the atom numbering scheme, showing 30% probability ellipsoids. Hydrogen atoms and solvent molecules are omitted for clarity.

In **3**, two monoatom bridged μ-SCN groups replace the OH groups in **1** and **2** to connect the three cobalt atoms (Figure 3). The lengths of the bonds of the central Co1 to the four centrosymmetric nitrogen atoms of pdz are 2.143(5) and 2.149(4) Å, and those to the two nitrogen atoms of μ-NCS are 2.125(4) Å. The terminal Co2 is coordinated to six nitrogen atoms: two from bridging pdz ligands, one from the μ-SCN group, one from the terminal pdz ligand, and another two from terminal NCS ligands. Differing from the close connections observed in **1** and **2**, the bond lengths of the cobalt atoms to the nitrogen atoms of the bridging NCS ligands are 2.125(4) (central Co) and 2.197(5) Å (terminal Co), which are longer than those to the terminal NCS ligands [2.056(7) and 2.041(5) Å, respectively]. The bridging pdz ligand in **3** affords two nitrogen donors with similar bond lengths [2.143(5) Å for Co1 and 2.192(4) Å for Co2] and angles [118.9(3) and 118.6(4)°] to

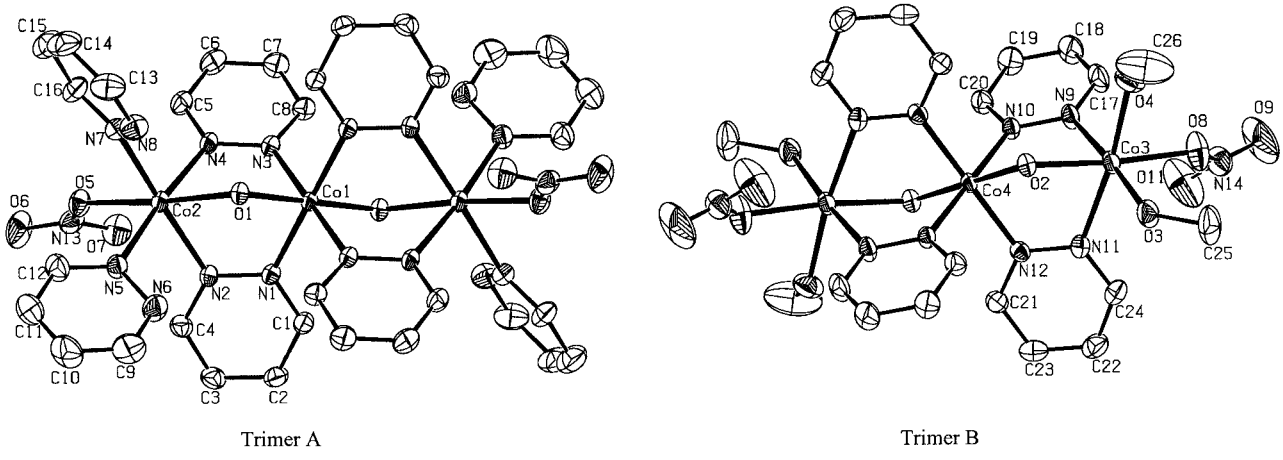

Figure 2. An ORTEP drawing of the two trimers in **2**, with the atom numbering scheme, showing 30% probability ellipsoids. Hydrogen atoms and uncoordinated anions are omitted for clarity.

the two adjacent metal atoms. The shortest intramolecular and intermolecular distances between the metal atoms are 3.43 and 8.55 Å, respectively, which are longer than those in **1** and **2**. Two uncoordinated methanol solvents are disordered in the molecular structure. A similar coordination sphere has been published for a nickel compound.[10]

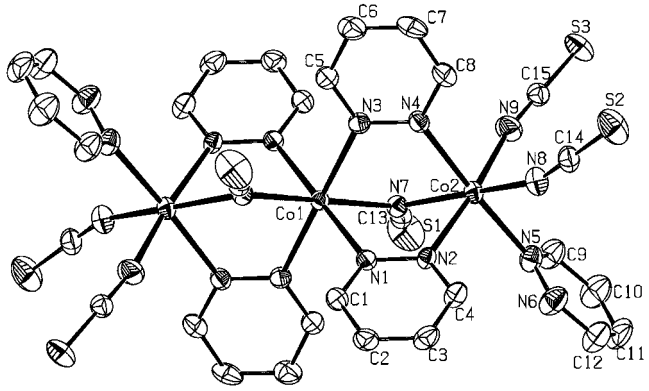

Figure 3. An ORTEP drawing of **3**, with the atom numbering scheme, showing 30% probability ellipsoids. Hydrogen atoms and solvent molecules are omitted for clarity.

As a bidentate bridging ligand, pdz can bond to different metal centers and display a variety of geometry and network motifs. The coordination modes of the pdz ligand could simply be summed up in three types according to the bridging methods. Type I is a typical monodentate mode as observed in the terminal ligands of multinuclear compounds, in which each pdz ligand only affords one nitrogen donor. The coordination type II is the typical bidentate bridging mode observed in **3** and other trinuclear or polymeric compounds,[5–9,13–15] in which the bridging pdz ligand affords two nitrogen donors symmetrically. Type III is the novel bridging mode first observed in **1** and **2**, in which the bond lengths between the two nitrogen atoms of the bridging pdz ligand and the two metal atoms are significantly different. It is obvious that the coordination mode of pdz is strongly affected by the second bridging ligand and the variety of bridging modes of pdz influences the magnetic properties of the compounds strongly.

Magnetic Properties

All the samples used for magnetic measurements were pulverized crystals. The anisotropic magnetic measurement was not carried out, because the crystals lost their solvent molecules when they were powdered. The magnetic measurements of the thermal variation of the magnetic susceptibility for **1** and **3**, plotted as $\chi_M T$ vs. temperature in the temperature range 2–300 K (2–250 K for **3**) are shown in Figure 4 and Figure 5, respectively (χ_M, the magnetic susceptibility per mole of trimer, was corrected for **1** by using the true molecular weight obtained from the elemental analysis). The $\chi_M T$ value for **1** at room temperature (5.19 $cm^3 \cdot K \cdot mol^{-1}$ at a magnetic field of 0.1 T) corresponds to that expected for two noninteracting high-spin cobalt atoms (S = 3/2) and one low-spin cobalt atom (S = 1/2), which is consistent with the results from the crystal structure data, in which the central Co atom is in a low-spin state with an average bond length of 1.93 Å, and the two terminal Co atoms are in a high-spin state with an average bond length of 2.09 Å. The $\chi_M T$ value remains practically unchanged down to 20 K, then decreases slightly, and finally increases quickly to 6.4 $cm^3 \cdot K \cdot mol^{-1}$ at 2 K under a magnetic field of 0.1 T, whereas at a magnetic field of 1 T, it goes through a maximum of 4.9 $cm^3 \cdot K \cdot mol^{-1}$ at 5.5 K and decreases again upon further cooling as a result of a field-saturation effect. The magnetic phenomenon in **1** can be explained by the irregular spin states structure, which has been reported in the $M^{II}Cu^{II}M^{II}$ (M = high-spin state of Mn, Co or Ni) system.[1,16] In the case of **1**, the interaction between Co(3/2) and Co(1/2) is weakly antiferromagnetic, the ground state is E(5/2, 3), above it there are E(7/2, 3), E(5/2, 2), E(3/2, 1), E(1/2, 0), E(1/2, 1), and E(3/2, 2). Such an irregular spin states structure exhibits quasi ferrimagnetic behavior in the $\chi_M T$ vs. T plots as shown in Figure 4.

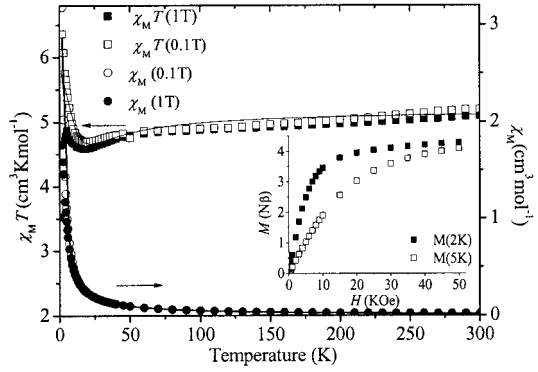

Figure 4. Thermal variation of $\chi_M T$ and χ_M for **1** at a magnetic field of 0.1 T (empty square and circle) and 1 T (filled square and circle), the solid line is the best fit for χ_M and $\chi_M T$ at 0.1 T using Equation (3). The inset is the magnetic field dependence of magnetization of **1** at temperatures of 2 and 5 K.

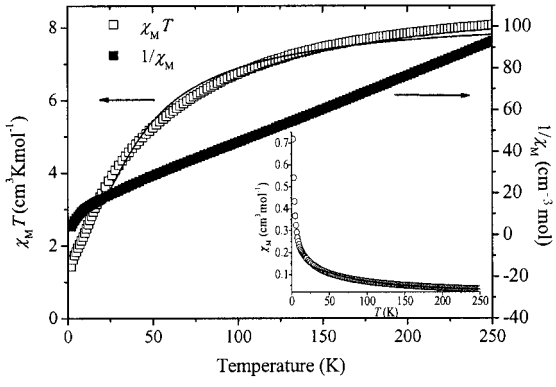

Figure 5. Thermal variations of $\chi_M T$ and $1/\chi_M$ for **3** at a magnetic field of 1 T. The inset is the curve of χ_M vs. T, and the solid line is the best fit for $\chi_M$and $\chi_M T$ using Equation (4).

To simulate the experimental magnetic behavior, the data of **1** and **3** are approximately fitted by the isotropic linear

trinuclear model.[1] The spin Hamiltonian and relative energies in the zero field are expressed as follows:

$$H = -J(S_{A1}.S_B + S_{A2}.S_B) \quad (1)$$

where $S_A = 3/2$, $S_B = 1/2$ for **1** and $S_A = S_B = 3/2$ for **3**.

$$E(S, S') = -(J/2)S(S+1) + (J/2)S'(S'+1);\ S' = S_{A1} + S_{A2},\ S = S' + S_B \quad (2)$$

The situation is always complicated for cobalt compounds. The exact expression of the Hamiltonian including spin-orbit coupling, axial and rhombic distortions, exchange, and Zeeman interactions[17] is not within the limits of our ability to calculate because of the very large size of the matrices. Therefore, the approximate fit for the average $\chi_M(T)$ [Equation (3)] was used for **1**, in which the orbital degeneracy on the distorted octahedral terminal Co^{II} ($^4T_{1g}$) and the zero-field splitting effects were ignored.[1,13] Considering the phenomenon of an ascending $\chi_M T$ value at low temperature, both the antiferromagnetic exchange, J, between the neighboring HS and LS cobalt atoms and the weak ferromagnetic exchange, J', between the two terminal cobalt atoms were included.

The best fit gives $g_A = 2.26$, $g_B = 2.04$, $J = -9.37\ cm^{-1}$, and $J' = 0.95\ cm^{-1}$ with $R = 3.9\cdot10^{-4}$ $\{R = \Sigma[(\chi_M T_{obs}) - (\chi_M T_{calc})]^2/\Sigma(\chi_M T_{obs}^2)\}$. The high values of g_A for the terminal cobalt atoms reflect the spin-orbit coupling effects and the orbital degeneracy of octahedral HS Co^{II}.[13,18] The J value is reasonably indicative of the exchange interactions across the pyridazine bridges.[13] The low-temperature limit of $\chi_M T$, $(\chi_M T)_{LT}$, is 5.736 $cm^3\cdot K\cdot mol^{-1}$, a little less than the value measured at 2 K (6.4 $cm^3\cdot K\cdot mol^{-1}$), which indicates an irregular spin states structure in **1** in the low-temperature range. If the temperature is low enough, the whole trimer is in the ground state with $S = 5/2$. The calculated saturation magnetization is 5.71 Nß at g (5/2, 3) = 2.29. The measured magnetization of **1** as a function of field (0–5 T) gives a saturation magnetization value of 4.27 Nß at 2 K (Figure 4, inset), which is less than the value of $S = 5/2$, which also proves that the magnetic behavior at low temperature is a result of an irregular spin states structure.

The $\chi_M T$ value per trimer of **3** at 250 K is 8.07 $cm^3\cdot K\cdot mol^{-1}$ (Figure 5), which is larger than that for three noninteracting cobalt ions of $S = 3/2$ because of the orbital contribution. This value decreases gradually to 0.48 $cm^3\cdot K\cdot mol^{-1}$ from room temperature to 2 K. The $1/\chi_M$ value above 20 K fitted with the Curie–Weiss law gave C = 3.016 $cm^3\cdot mol^{-1}$ and $\theta = -32.09$ K, which shows an intramolecular antiferromagnetic coupling of the adjacent cobalt atoms within the trimer. With the same approximations as in **1** and neglecting J', the *Van Vleck* formula for **3** is expressed in Equation (4).

The best fit for temperatures greater than 20 K gives g_A = 2.46, g_B = 2.02, $J = -6.08\ cm^{-1}$ with $R = 9.5\cdot10^{-4}$. The larger value of g_A indicates that the terminal cobalt atoms possess stronger anisotropy than the central one, which is consistent with the description of the molecular structure.

According to the theoretical calculations of magnetic interactions through bridged two-atom pdz and related compounds,[5,6,10,13] the magnetic coupling of the two cobalt atoms through pure bridging pdz ligands ($J \approx -10\ cm^{-1}$) are much weaker than that in the copper ($-J > 100\ cm^{-1}$) and nickel ($J \approx -30\ cm^{-1}$) compounds. It can be estimated that the contribution to the antiferromagnetic interaction between the adjacent cobalt atoms mainly comes from the bridging pdz ligands in **3**. End-on NCS^- bridging may afford a weak ferromagnetic interaction, which compensates the antiferromagnetic interaction through the bridging pdz ligands to give a comparatively small value of J, as described for the corresponding nickel compound.[10] In the case of **1**, the entire magnetic interaction of the adjacent HS and LS cobalt atoms comes from the magnetic coupling through pdz and hydroxide, and the supra-exchange of the two metal ions. It can be deduced that the magnetic coupling through pdz must be an antiferromagnetic interaction

$$\chi_M = \frac{N\beta^2}{4kT} \times \frac{35g^2_{(5/2,3)} + 84g^2_{(7/2,3)}\exp(\frac{7J}{2kT}) + 35g^2_{(5/2,2)}\exp(\frac{3J-3J'}{kT}) + 10g^2_{(3/2,2)}\exp(\frac{J-6J'}{2kT}) + 10g^2_{(3/2,1)}\exp(\frac{5J-10J'}{2kT}) + g^2_{(1/2,1)}\exp(\frac{J-5J'}{kT}) + g^2_{(1/2,0)}\exp(\frac{2J-6J'}{kT})}{3 + 4\exp(\frac{7J}{2kT}) + 3\exp(\frac{3J-3J'}{kT}) + 2\exp(\frac{J-6J'}{2kT}) + 2\exp(\frac{5J-10J'}{2kT}) + \exp(\frac{J-5J'}{kT}) + \exp(\frac{2J-6J'}{kT})} \quad (3)$$

$$\chi_M = \frac{N\beta^2}{4kT} \times \frac{10g^2_{(3/2,3)} + 10g^2_{(3/2,0)}\exp(\frac{6J}{kT}) + g^2_{(1/2,1)}\exp(\frac{7J}{2kT}) + 35g^2_{(5/2,1)}\exp(\frac{15J}{2kT}) + g^2_{(1/2,2)}\exp(\frac{3J}{2kT}) + 84g^2_{(7/2,2)}\exp(\frac{9J}{kT}) + 165g^2_{(9/2,3)}\exp(\frac{21J}{2kT})}{2 + 2\exp(\frac{6J}{kT}) + \exp(\frac{7J}{2kT}) + 3\exp(\frac{15J}{2kT}) + \exp(\frac{3}{2}J/kT) + 4\exp(\frac{9J}{kT}) + 5\exp(\frac{21J}{2kT})} \quad (4)$$

because of spin polarization in the bridging ligand. The antiferromagnetic coupling between two neighboring cobalt atoms through the OH^- group is very weak because of poor overlap between the $d_{x^2-y^2}$ and d_{z^2} magnetic orbitals of the central low-spin cobalt(II) atom and the p-type orbitals of the oxygen atom from the OH^- group. The different magnetic orbital contributions for the high- and low-spin states of the cobalt atoms also cause the overlap of the electron clouds of the two neighboring metal atoms to tend to zero and the spins of the two high-spin magnetic centers to tend to be positioned in the same direction, compensating for the antiferromagnetic interaction between neighboring cobalt atoms. The magnetic exchange for the two kinds of spin states of cobalt atoms within one molecule is rarely reported. The tuning of the spin states through a simple bridging ligand may afford a new method for the modification of magnetic properties at the molecular level.

In conclusion, three novel cobalt(II) trinuclear compounds bridged by the pdz ligand and a second small anion (hydroxide and end-on thiocyanate) were structurally and magnetically characterized in this paper. The two-atom bridging modes of the pdz ligand in **1** and **2** are unusual: each bridging pdz ligand affords two nitrogen donors to the two metal ions with different bond lengths. This results in a significant difference in the ligand fields between the central and terminal cobalt(II) coordination spheres in **1** and **2**. Both the structural analysis and magnetic data show that two spin states (HS and LS) of cobalt(II) atoms coexist in **1**. An irregular spin states structure was also observed in this compound at low temperature. This work provides a unique example of the modification of magnetic properties through a simple bridging group.

Experimental Section

Materials: $Co(NO_3)_2{\cdot}6H_2O$ (>98%, Wako), pyridazine (98%, Tokyo Chemical), NH_4SCN (99.5%, Wako) were used as obtained from commercial sources without further purification.

Physical Measurements: The powder infrared spectra were recorded with a Perkin–Elmer System 2000 instrument using KBr pellets. Magnetic susceptibility measurements were carried out using a Quantum Design SQUID magnetometer in the 2–300-K temperature range. Corrections for diamagnetism were applied by using Pascal's constants.[1a]

Synthesis of $[Co_3(\mu\text{-}OH)_2(\mu\text{-}pdz)_4(pdz)_2(NO_3)_2(H_2O)_2]{\cdot}(NO_3)_2{\cdot}(THF){\cdot}2(MeOH)$ (1) and $[Co_3(\mu\text{-}OH)_2(\mu\text{-}pdz)_4(pdz)_4(NO_3)_2]{\cdot}[Co_3(\mu\text{-}OH)_2(\mu\text{-}pdz)_4(MeOH)_4(NO_3)_2]{\cdot}(NO_3)_4$ (2): After mixing a THF solution (5 mL) of pdz (1.1 mmol) and a THF solution (15 mL) of $Co(NO_3)_2{\cdot}6H_2O$ (0.5 mmol), a red sediment was produced, which was dissolved by adding methanol (5 mL). Red-brown, cube-shaped single crystals of **1** were obtained from the prepared red solution by slow vaporization at room temperature. The crystals lost their solvent molecules and powdered slowly in air. $C_{30}H_{46}Co_3N_{16}O_{19}$ (**1**): calcd. C 32.39, H 4.14, N 20.15; found C 27.55, H 3.38, N 21.47. The experimental data is consistent with that of the molecule in which three organic solvent molecules are replaced by four water molecules. $C_{24}H_{38}Co_3N_{16}O_{20}$ (**1** – THF – 2MeOH + $4H_2O$): found C 27.52, H 3.66, N 21.40. Pyramid-shaped red crystals of **2** were isolated after one year from the same mother liquor of **1**. $C_{52}H_{64}Co_6N_{34}O_{38}$ (**2**): calcd. C 29.37, H 3.03, N 22.39; found C 29.58, H 3.25, N 22.13.

Synthesis of $[Co_3(\mu\text{-}pdz)_4(\mu\text{-}NCS)_2(pdz)_2(NCS)_4]{\cdot}2MeOH$ (3): Pyridazine (2.2 mmol) was added dropwise to a solution of $CoCl_2{\cdot}6H_2O$ (1 mmol) and NH_4SCN (2.2 mmol) in methanol (20 mL) under continuous stirring. The prepared blue solution was filtered and allowed to evaporate slowly at room temperature to give red cube-shaped single crystals of **3** after two months. IR

Table 2. Crystallographic data for **1**, **2**, and **3**.

	1	**2**	**3**
Formula	$C_{30}Co_3H_{46}N_{16}O_{19}$	$C_{26}H_{32}Co_3N_{17}O_{19}$	$C_{32}H_{30}Co_3N_{18}O_2S_6$
Fw	1111.56	1063.44	1067.87
Dimensions [mm]	0.25×0.20×0.15	0.3×0.20×0.1	0.25×0.20×0.1
Crystal system	monoclinic	triclinic	monoclinic
Space group	*P*21/c	$P\bar{1}$	*P*21/*n*
a [Å]	10.115(1)	12.8257(5)	15.307(2)
b [Å]	18.437(1)	12.950(1)	11.1583(5)
c [Å]	12.573(1)	13.5136(5)	14.983(3)
α [°]		74.499(2)	
β [°]	113.777(2)	71.412(3)	117.337(2)
γ [°]		85.829(2)	
V [Å^3]	2145.6(3)	2049.8(2)	2273.3(5)
Z	2	2	2
$\rho_{cal\ d.}$ [g·cm^{-3}]	1.714	1.723	1.560
μ [cm^{-1}]	12.43	12.98	14.10
Temperature [°C]	293	293	293
No. of observations	2464	7066	3759
h	$-10 < h < 10$	$-16 < h < 15$	$-19 < h < 11$
k	$-19 < k < 15$	$-10 < k < 16$	$-14 < k < 10$
l	$-13 < l < 12$	$-17 < l < 17$	$-11 < l < 19$
Residuals:[a] *R*,[b] wR_2	0.031, 0.077	0.07, 0.2123	0.0705, 0.2011
GoF	1.06	1.194	1.298
Max. & min. peak in final diff. map (e$^-$ [Å^3])	0.45, –0.52	1.12 (0.72 Å from Co3), –0.78	0.62, –0.56

[a] $R = \Sigma||F_{obsd.}| - |F_{calcd.}||/\Sigma|F_{obsd.}|$ for $I > 2.0\sigma(I)$. [b] $Rw = [\Sigma w\,(|F_{obsd.}| - |F_{calcd.}|)^2/\Sigma w\,F_o^2]^{1/2}$.

(KBr): $\tilde{\nu}$ = 3388 (br., m), 3092 (br., w), 2079 (vs), 1989 (s), 1579 (m), 1415 (m), 1070 (m), 991 (w), 767 (m), 673 (w), 412 (w) cm^{-1}. $C_{32}H_{30}Co_3N_{18}O_2S_6$: calcd C 35.96, H 2.81, N 23.60, found C 35.35, H 2.87, N 23.67.

X-ray Crystallography

The single crystals of all the compounds were sealed into glass capillary tubes (0.7 mm, GLAS) containing a small amount of mother liquor and mounted on the crystal goniometer. The intensity data of all four samples were collected with the Rigaku Mercury CCD system using graphite monochromatic Mo-K_α radiation (λ = 0.71069 Å) and the ω scan technique with a sample-to-detector distance of 35 mm at a temperature of 20 ± 1 °C (Table 2). The cell constants and orientation matrix were obtained from the reflections collected on the setting angles of six frames by changing ω by 0.5° for each frame.[19] Intensity data were collected in 480 frames with an ω scan width of 0.5° using two different ψ settings (0 and 90°). The exposure time was 60, 90, and 150 s for **1**, **2**, and **3**, respectively. Empirical absorption corrections based on azimuthal scans were applied.[20] The data were also corrected for Lorentz and polarization effects.

All calculations were performed using the teXsan crystallographic software package[21] of the Molecular Structure Corporation. The structures were solved by direct methods and expanded using Fourier techniques.[22] The full-matrix least-squares refinement was performed by SHELXL-97[23] based on F^2. The non-hydrogen atoms were refined anisotropically. Hydrogen atoms were included but not refined. R factor (gt) of the final full-matrix least-squares refinement was based on the observed data of $I > 2\sigma(I)$, while reflections of the weighted R factor (wR_2) and GoF are based on all data. In **1** and **3**, the positions of the solvent molecules were disordered, while in **2**, the oxygen atoms of the terminally coordinated NO_3^- were disordered. CCDC-276336 to 276338 contain the supplementary crystallographic data for this paper. These data can be obtained free of charge from The Cambridge Crystallographic Data Centre via www.ccdc.cam.ac.uk/data_request/cif.

Acknowledgments

This work was supported by the Japanese Society for the Promotion of Science (JSPS) and the National Science Foundation of China (NSFC 20441006).

[1] a) O. Kahn, *Molecular Magnetism*, VCH, Weinheim, Germany, **1993**; b) *Magnetism: A Supramolecular Function*, ASI Kluwer Academic Publishers, **1995**.
[2] J. V. C. Rovira, D. B. Amabilino, *Supramolecular Engineering of Synthetic Metallic Materials*, Kluwer Academic Publishers, **1999**.
[3] K. Itoh, M. Kinoshita, *Molecular Magnetism-New Magnetic Material*, Gordon and Breach Science Publishers, **2000**.
[4] For example: a) S. Ferlay, T. Mallah, R. Ouahès, P. Veillet, M. Verdaguer, *Nature* **1995**, *378*, 701–703; b) O. Sato, T. Iyoda, A. Fijishma, K. Hashimoto, *Science* **1996**, *272*, 704–705; c) O. Kahn, C. Jay Martinez, *Science* **1998**, *279–282*, 44–48.
[5] a) L. Carlucci, G. Ciani, M. Moret, A. Sironi, *J. Chem. Soc., Dalton Trans.* **1994**, 2397–2403; b) T. Otieno, S. J. Rettig, R. C. Thompson, J. Trotter, *Inorg. Chem.* **1995**, *34*, 1718–1725.
[6] a) L.-Q. Chen, L. K. Thompson, J. N. Bridson, *Inorg. Chim. Acta* **1996**, *244*, 87–93; b) L. K. Thompson, S. K. Mandal, E. J. Gabe, F. L. Lee, A. W. Addison, *Inorg. Chem.* **1987**, *26*, 657–664; c) L. K. Thompson, A. W. Hanson, B. S. Ramaswamy, *Inorg. Chem.* **1984**, *23*, 2459–2465.
[7] a) J. Manzur, A. M. Garcia, R. Letelier, E. Spodine, O. Pena, D. Grandjean, M. M. Olmstead, B. C. Noll, *J. Chem. Soc., Dalton Trans.* **1993**, 905–911; b) Zh.-Q. Xu, L. K. Thompson, C. J. Matthews, D. O. Miller, A. E. Geota, C. Wilson, J. A. K. Howard, M. Ohba, H. Okawa, *J. Chem. Soc., Dalton Trans.* **2000**, 69–77.
[8] A. Escuer, R. Vicente, B. Mernari, A. El Gueddi, M. Pierrot, *Inorg. Chem.* **1997**, *36*, 2511–2516.
[9] T. Wen, L. K. Thompson, F. L. Lee, E. J. Gabe, *Inorg. Chem.* **1988**, *27*, 4190–4196.
[10] J. Cano, G. De Munno, F. Lloret, M. Julve, *Inorg. Chem.* **2000**, *39*, 1611–1614.
[11] F. A. Cotton, G. Wilkinson, *Advanced Inorganic Chemistry*, John Wiley & Sons, New York, **1988**.
[12] J. F. Berry, F. A. Cotton, C. Y. Liu, T. B. Lu, C. A. Murillo, B. S. Tsukerblat, D. Villagran, X. P. Wang, *J. Am. Chem. Soc.* **2005**, *127*, 4895–4902.
[13] a) S. Brooker, D. J. de Geest, R. J. Kelly, P. G. Plieger, B. Moubaraki, K. S. Murray, G. B. Jameson, *J. Chem. Soc., Dalton Trans.* **2002**, 2080–2087; b) U. Beckmann, S. Brooker, *Coord. Chem. Rev.* **2003**, *245*, 17–19.
[14] M. G. B. Drew, F. S. Esho, A. Lavery, S. M. Nelson, *J. Chem. Soc., Dalton Trans.* **1984**, 545–556.
[15] T. Yi, H.-Ch. Chang, S. Kitagawa, *Mol. Cryst. Liq. Cryst.* **2001**, *376*, 283–288.
[16] a) E. Q. Gao, J. K. Tang, D. Z. Liao, Z. H. Jiang, S. P. Yan, G. L. Wang, *Inorg. Chem.* **2001**, *40*, 3134–3140; b) P. Yu, J. Yves, O. Kahn, *Inorg. Chem.* **1988**, *27*, 399–404.
[17] a) R. Boca, *Coord. Chem. Rev.* **2004**, *248*, 757–815; b) A. V. Palii, B. S. Tsukerblat, E. Coronada, J. M. Clement-Juan, J. Borras-Almenar, *Inorg. Chem.* **2003**, *42*, 2455–2458; c) H. Sakiyama, R. Ito, H. Kumagai, K. Inoue, M. Sakamoto, Y. Nishida, M. Yamasaki, *Eur. J. Inorg. Chem.* **2001**, 2027–2032; H. Sakiyama, R. Ito, H. Kumagai, K. Inoue, M. Sakamoto, Y. Nishida, M. Yamasaki, *Eur. J. Inorg. Chem.* **2001**, 2705; d) K. Fink, C. Wang, V. Staemmler, *Inorg. Chem.* **1999**, *38*, 3847–3856.
[18] G. De Munno, M. Julve, F. Lloret, J. Faus, A. Caneschi, *J. Chem. Soc., Dalton Trans.* **1994**, 1175–1183.
[19] H.-Ch. Chang, H. Miyasaka, S. Kitagawa, *Inorg. Chem.* **2001**, *40*, 146–156.
[20] R. A. Jacobson, *REQABA Empirical Absorption Correction Version, 1.1–03101998*, Molecular Structure Corp., The Woodlands, TX, **1996–1998**.
[21] (*teXsan*): *Crystal Structure Analysis Package*, Molecular Structure Corporation, **1985** & **1999**.
[22] (*SIR92*): A. Altomare, M. C. Burla, M. Camalli, M. Cascarano, C. Giacovazzo, A. Guagliardi, G. Polidori, *J. Appl. Crystallogr.* **1994**, *27*, 435.
[23] G. M. Sheldrick, *SHELXL-97, An Integrated System for Solving and Refining Crystal Structures from Diffraction Data*, University of Göttingen, Germany, **1997**.

Received: August 22, 2005
Published Online: February 21, 2005

